Trigonometric Parallaxes of Star Forming Regions in the Scutum Spiral Arm

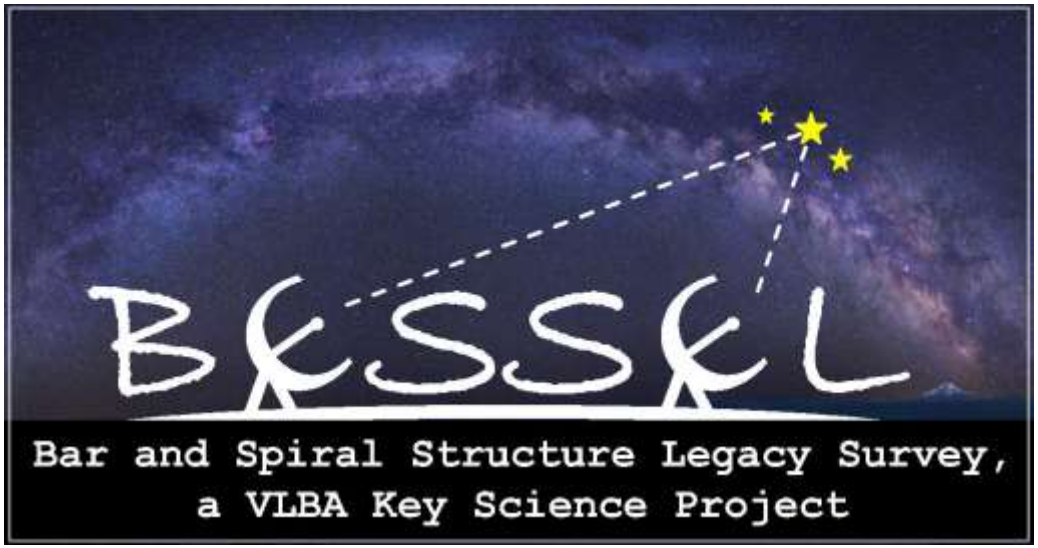

Jingjing Li

Purple Mountain Observatory

Collaborators: K. Immer, M. J. Reid, T. M. Dame, Y. Xu, A. Brunthaler, K.M.Menten et al.

2017-09-05 Cagliari

More than 100 models of the Milky Way

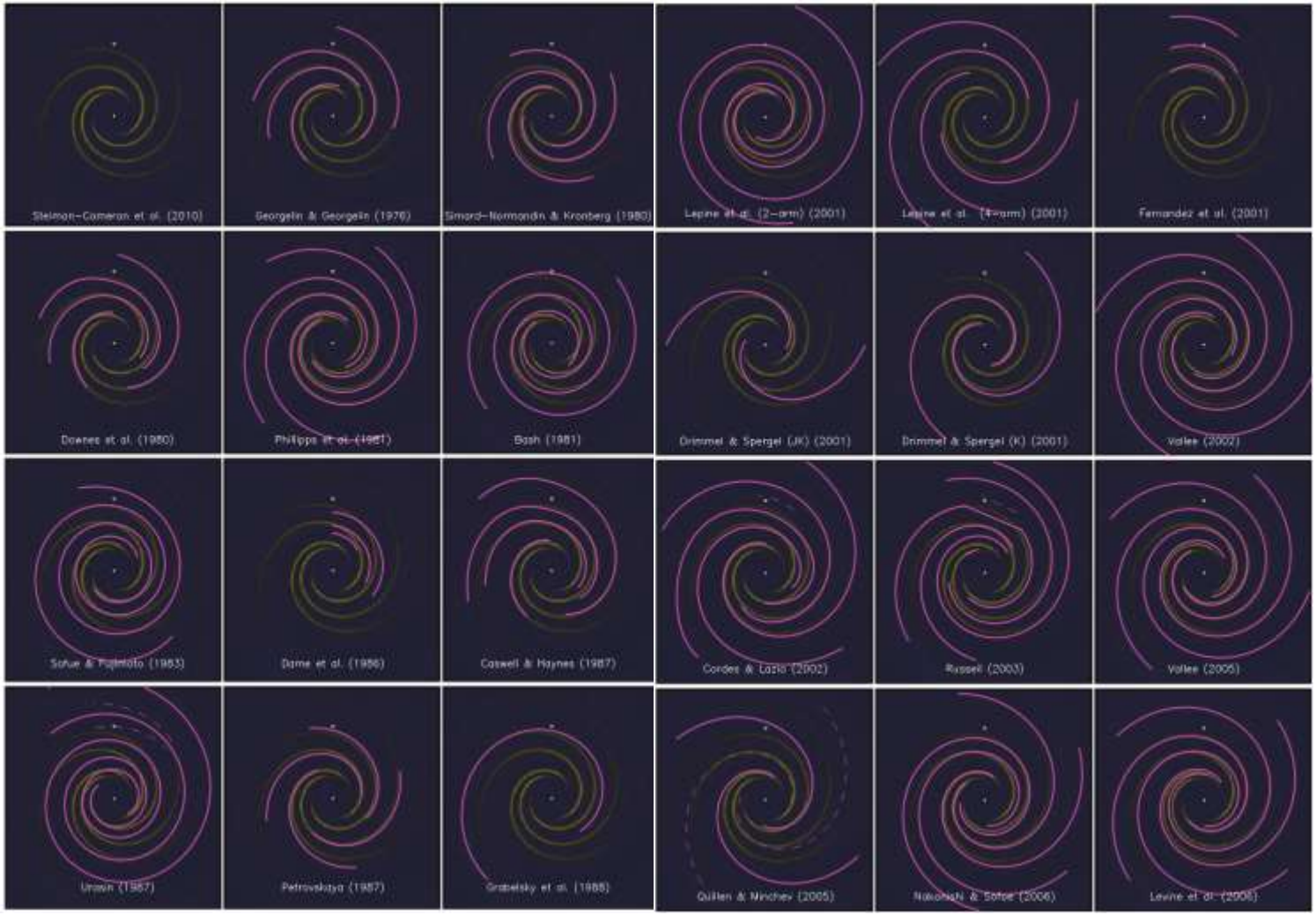

Reason: Lack of accurate distances to massive star-forming regions that trace spiral arm.

Large distance uncertainty

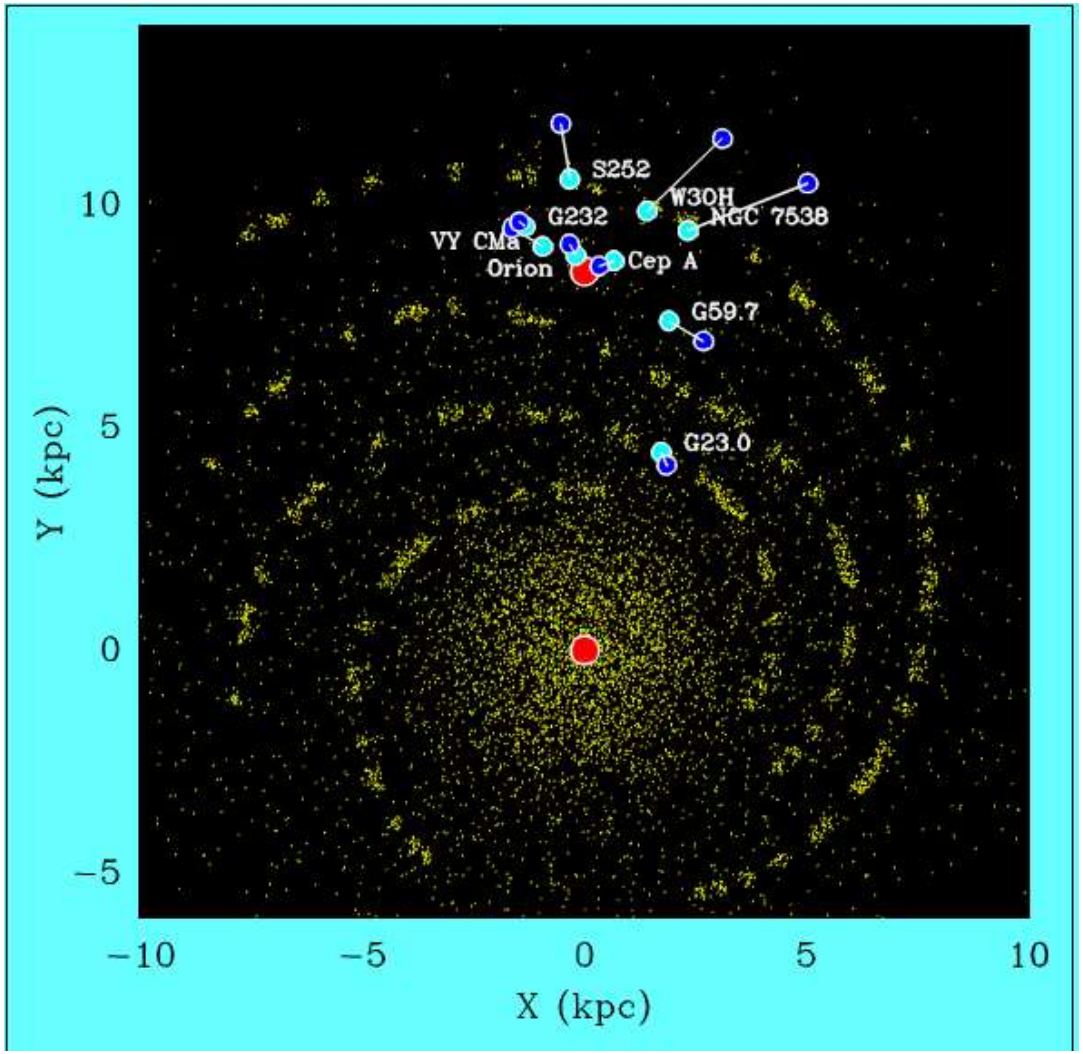

Reid et al. 2009

Moscadelli et al. 2009

Xu et al. 2009

Zhang et al. 2009

Brunthaler et al. 2009

BeSSeL & VERA Survey

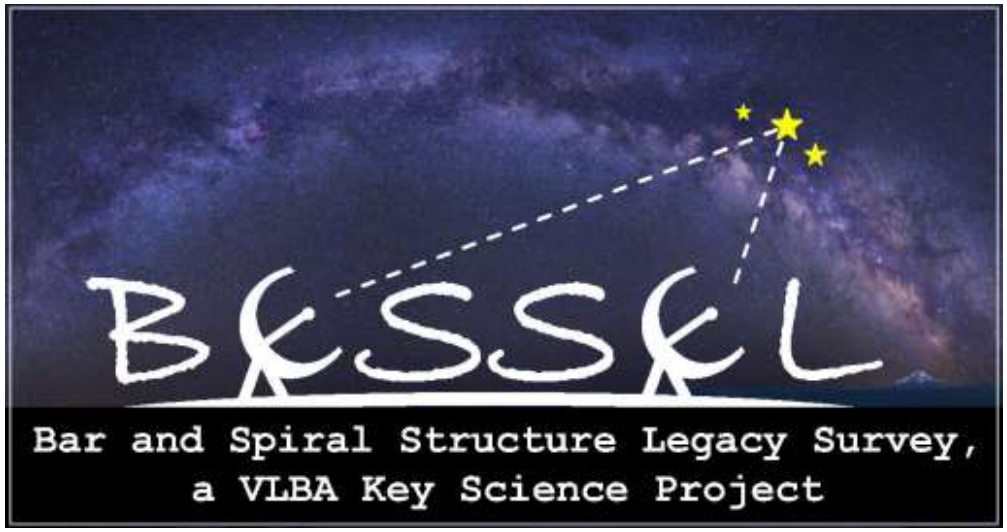

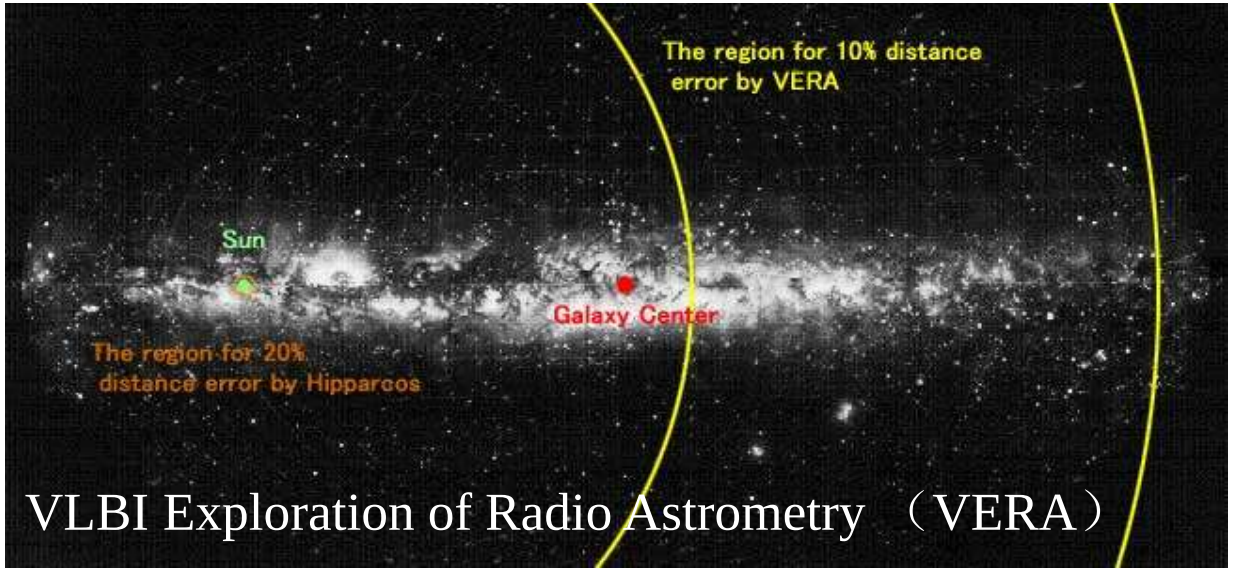

VLBI Exploration of Radio Astrometry （VERA）

What does the Scutum arm look like ?

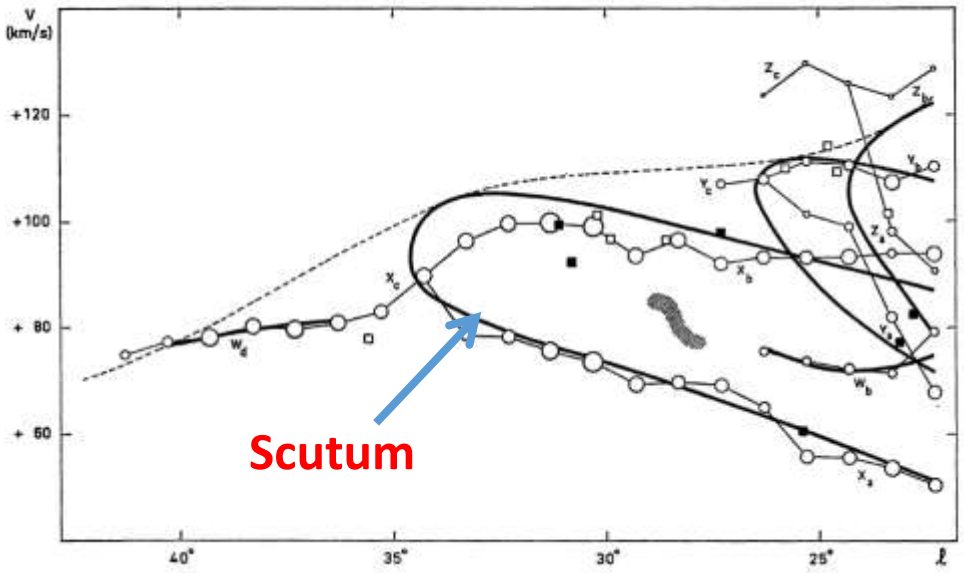

the locus of HI emission in *l* - V diagram
Shane et al. 1972

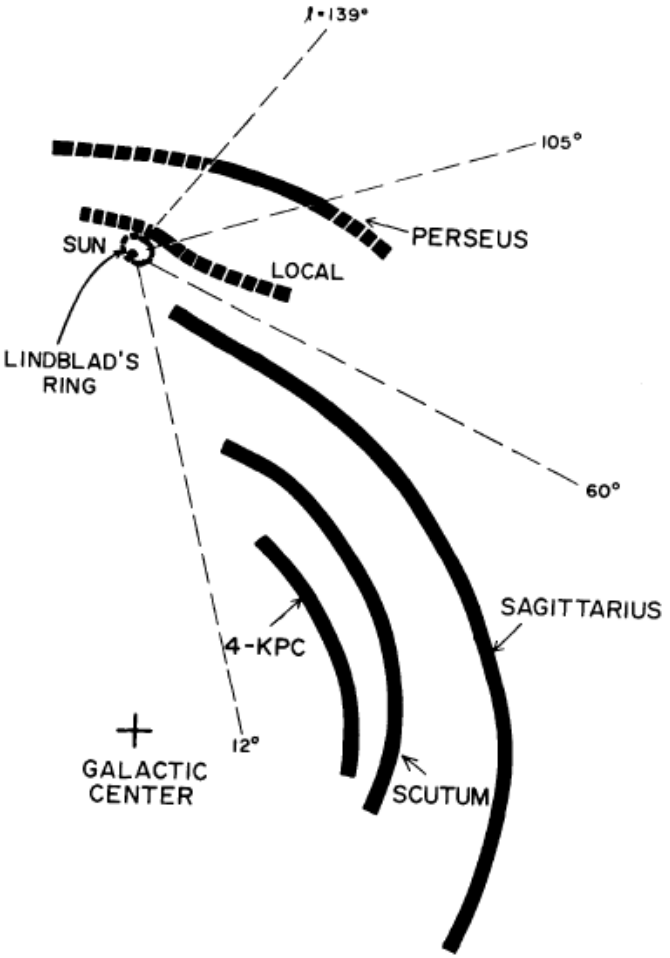

Cohen et al. 1980

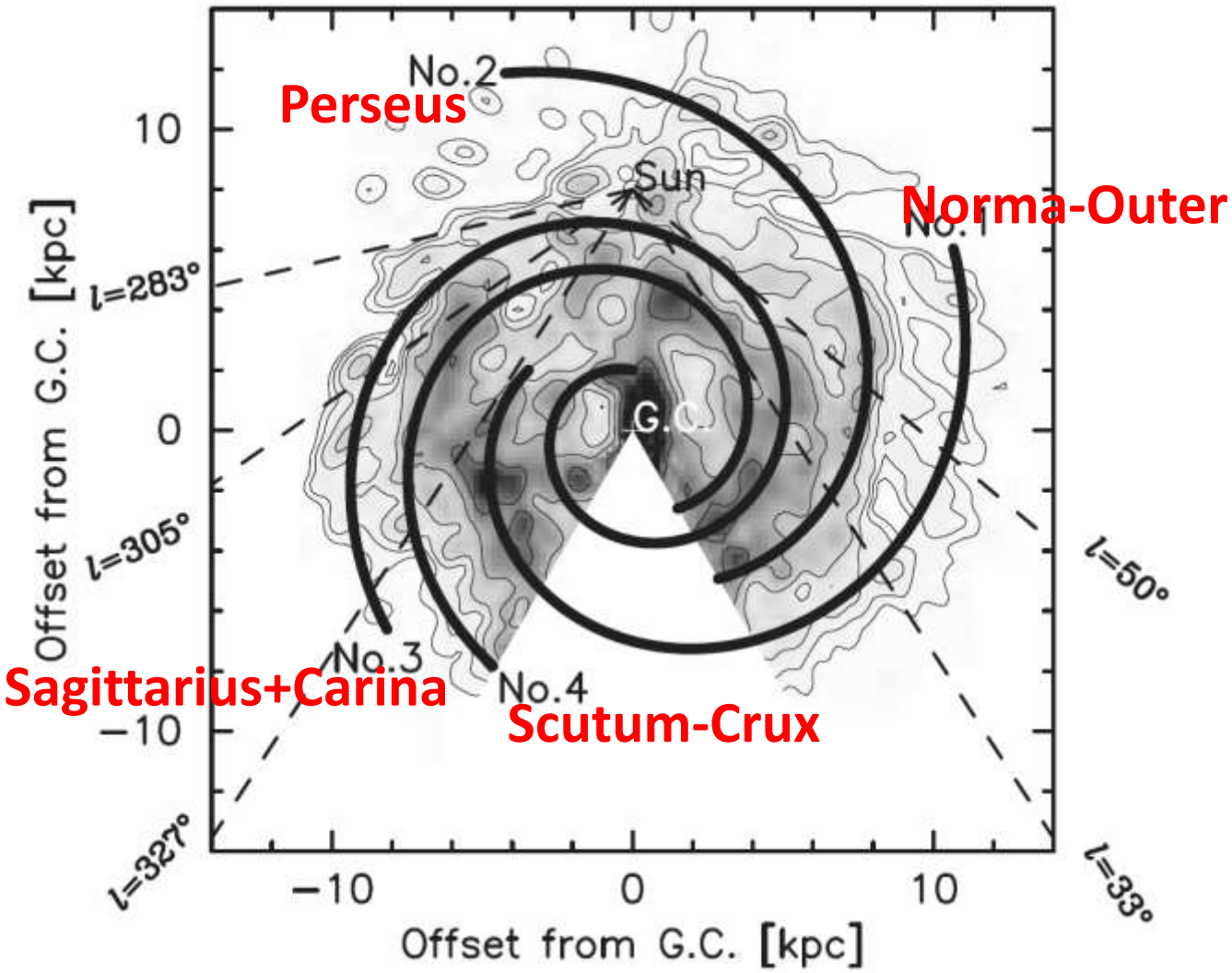

CO emission Nakanishi & Sofue 2006

The Galactic Molecular Ring (GMR) seems to consist of two spiral arms， the Sagittarius and Scutum arm.

The possible extension of the Scutum Arm

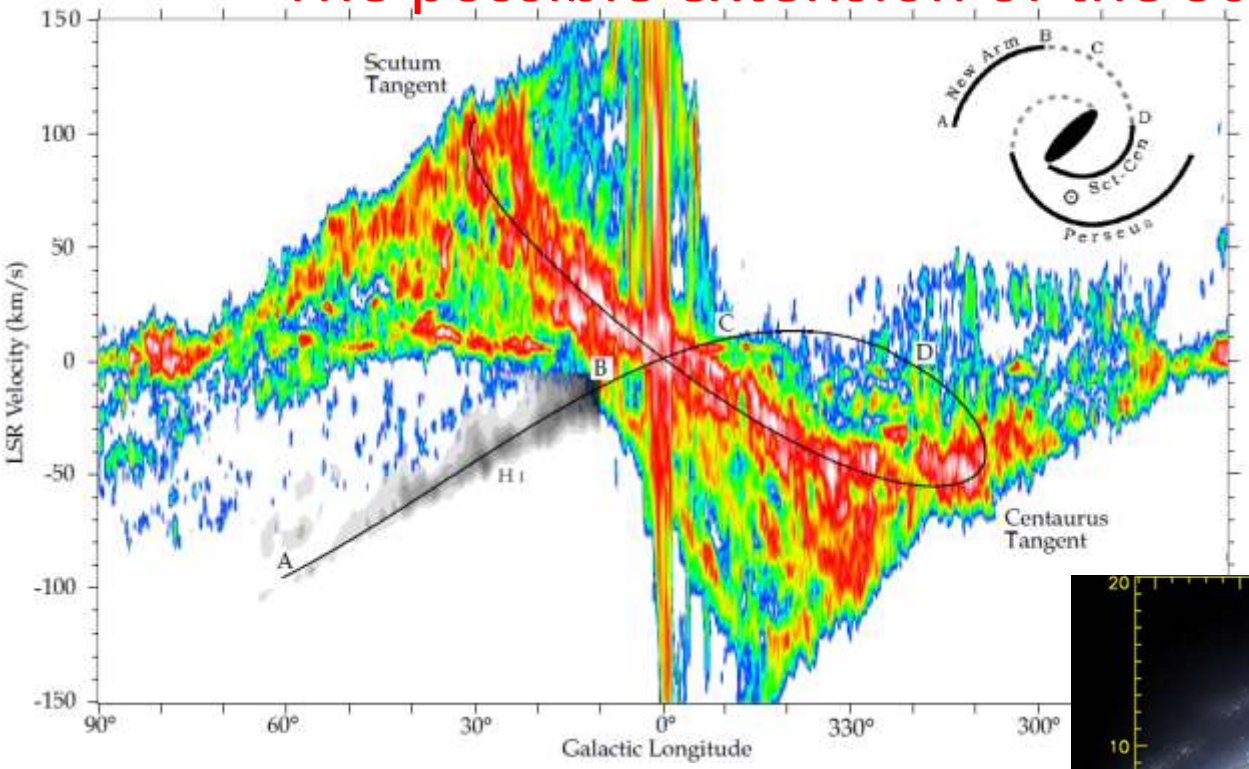

Dame et al. 2011

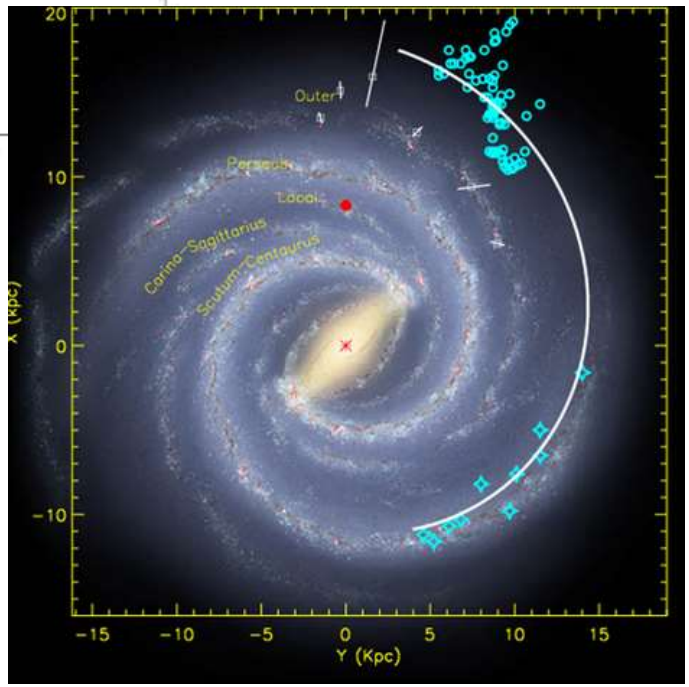

Sun et al. 2015

The Scutum Arm may extend from the end of the bar to outer second quadrant.

Observation

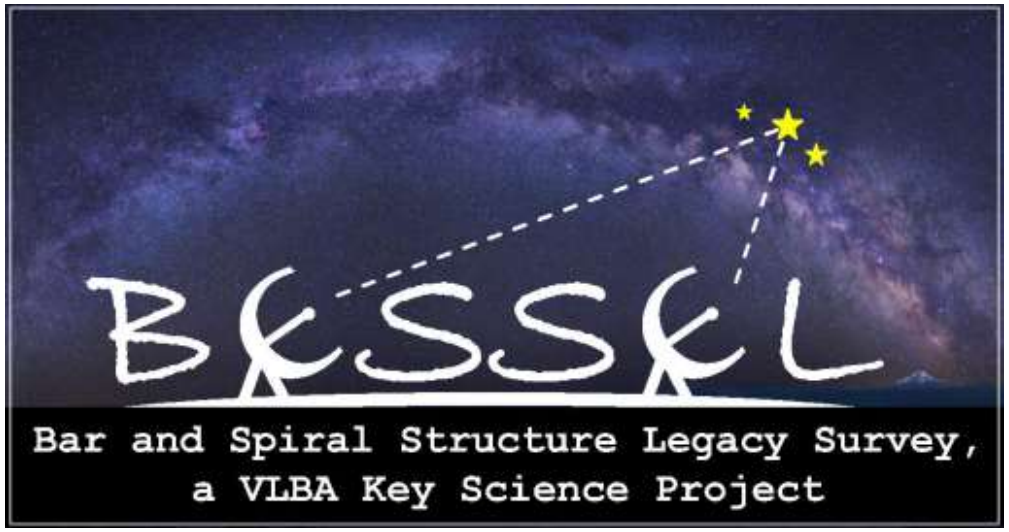

2012-2015 BR149 & BR198

22 GHz H_2O & 6.7 GHz CH_3OH masers

Techniques for Accurate Parallax Measurements for 6.7-GHz Methanol Masers (Reid et al. 2017)

Example: G28.14-0.00

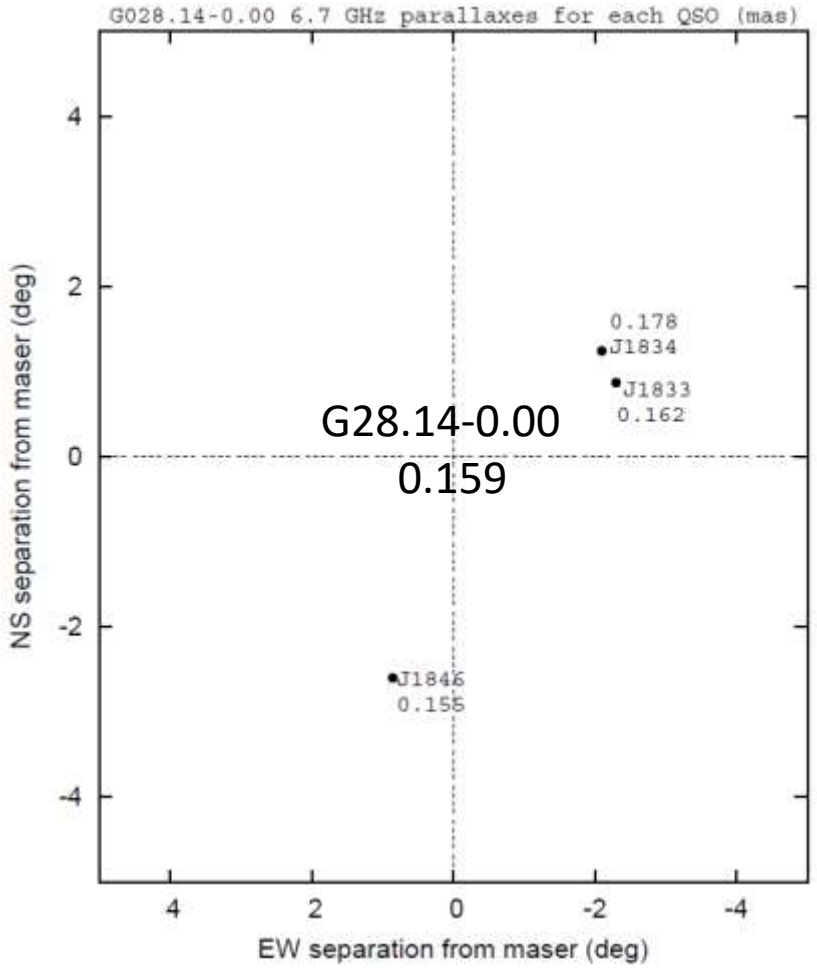

In order to deal with the problem of position gradients, we generate position data relative to an "artificial quasar" at the target maser position at each epoch. And then fit parallax to these data.

Example: G28.14-0.00

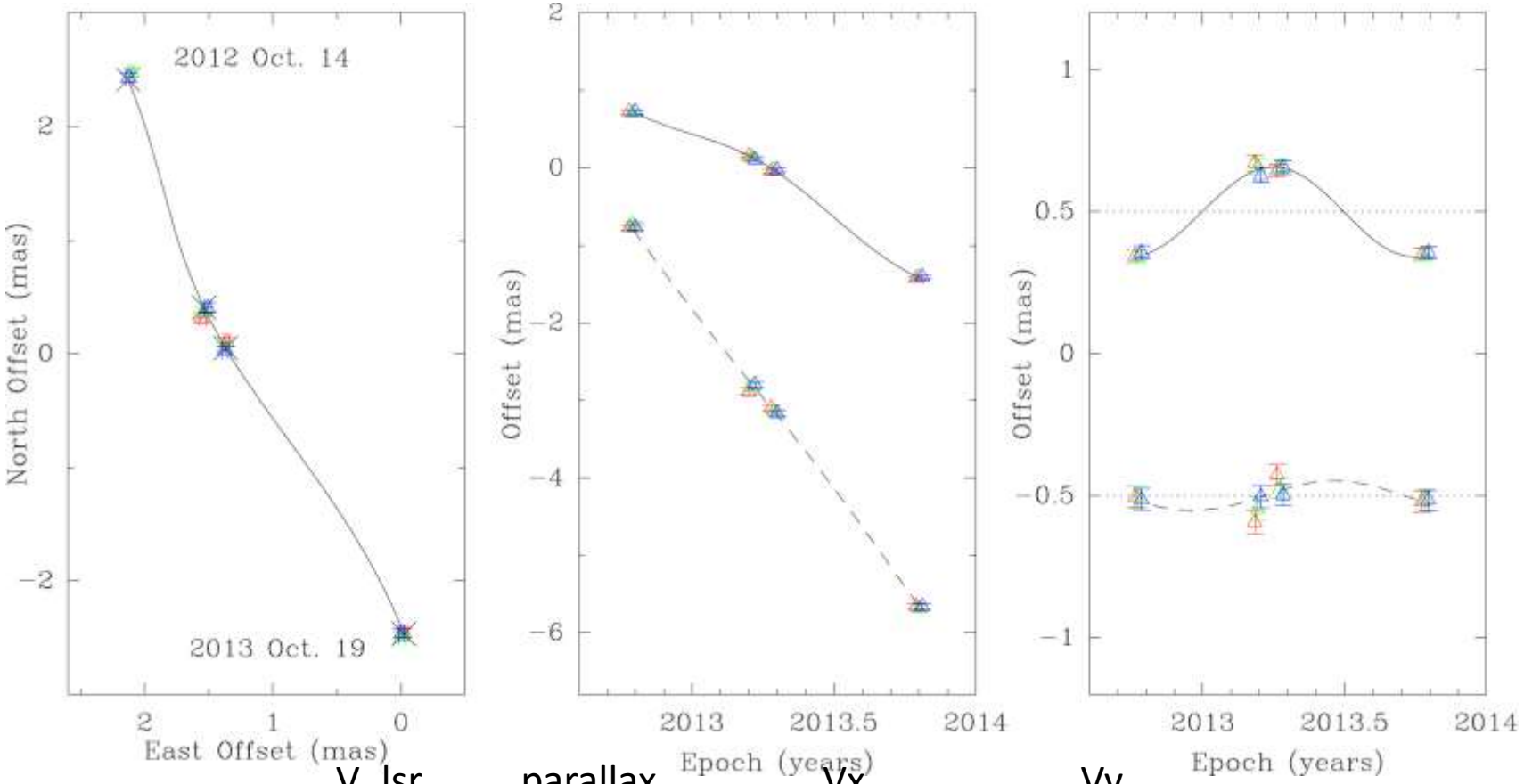

for artificial quasar:

V_lsr (km/s)	parallax (mas)	Vx (mas/yr)	Vy (mas/yr)
101.4	0.149(0.016)	-2.11(0.04)	-4.84(0.05)
101.0	0.163(0.016)	-2.10(0.04)	-4.90(0.05)
99.9	0.163(0.016)	-2.13(0.04)	-4.82(0.12)
combine	0.159(0.016)		
		-2.11(0.04)	-4.85(0.07)

Table 1. Parallaxes and Proper Motions of the Scutum Arm.

Source	R.A. (J2000) (h m s)	Dec. (J2000) (° ′ ″)	ϖ (mas)	μ_x (mas y^{-1})	μ_y (mas y^{-1})	$V_{\rm LSR}$ (km s^{-1})
G000.31 − 00.20	17 47 09.11	−28 46 16.3	0.356±0.024	0.19 ± 0.20	−1.81 ± 0.55	18 ± 3
G005.88 − 00.39	18 00 30.31	−24 04 04.5	0.334±0.020	0.18 ± 0.34	−2.26 ± 0.34	9 ± 3
G009.21 − 00.20	18 06 52.84	−21 04 27.9	0.355±0.028	−0.71 ± 0.07	−2.21 ± 0.52	43 ± 5
G010.32 − 00.15	18 09 01.45	−20 05 07.9	0.321±0.040	−0.80 ± 0.40	−1.80 ± 0.20	9 ± 5
G011.10 − 00.11	18 10 28.25	−19 22 30.2	0.364±0.027	−0.20 ± 0.05	−2.00 ± 0.15	29 ± 5
G011.91 − 00.61	18 13 58.12	−18 54 20.3	0.297±0.031	0.66 ± 0.28	−1.36 ± 0.41	37 ± 5
G012.68 − 00.18	18 13 54.75	−18 01 46.6	0.416±0.028	−1.00 ± 0.95	−2.85 ± 0.95	58 ± 10
G012.80 − 00.20	18 14 14.23	−17 55 40.5	0.343±0.037	−0.60 ± 0.70	−0.99 ± 0.70	34 ± 5
G012.88 + 00.48	18 11 51.42	−17 31 29.0	0.400±0.040	0.15 ± 0.25	−2.30 ± 0.39	31 ± 7
G012.90 − 00.24	18 14 34.42	−17 51 51.9	0.408±0.025	0.19 ± 0.80	−2.52 ± 0.80	36 ± 10
G012.90 − 00.26	18 14 39.57	−17 52 00.4	0.396±0.032	−0.36 ± 0.80	−2.22 ± 0.80	39 ± 10
G013.87 + 00.28	18 14 35.83	−16 45 35.9	0.254±0.024	−0.25 ± 2.00	−2.49 ± 2.00	48 ± 10
G016.58 − 00.05	18 21 09.08	−14 31 48.8	0.279±0.023	−1.13 ± 0.34	−2.59 ± 0.35	60 ± 5
G018.87 + 00.05	18 25 11.35	−12 27 36.5	0.297±0.020	−0.17 ± 0.06	−1.90 ± 0.21	39 ± 3
G023.25 − 00.24	18 34 31.24	−08 42 47.3	0.166±0.088	−1.70 ± 0.15	−4.30 ± 0.20	63 ± 5
G023.65 − 00.12	18 34 51.59	−08 18 21.4	0.313±0.039	−1.32 ± 0.20	−2.96 ± 0.20	81 ± 3
G024.63 − 00.32	18 37 22.71	−07 31 42.1	0.243±0.062	−0.31 ± 0.14	−2.98 ± 0.33	43 ± 5
G025.70 + 00.04	18 38 03.14	−06 24 15.2	0.098±0.029	−2.89 ± 0.07	−6.20 ± 0.36	93 ± 5
G027.36 − 00.16	18 41 51.06	−05 01 43.4	0.125±0.042	−1.81 ± 0.11	−4.11 ± 0.27	92 ± 3
G028.14 − 00.00	18 42 42.59	−04 15 35.1	0.159±0.016	−2.11 ± 0.04	−4.85 ± 0.07	100 ± 5
G028.30 − 00.38	18 44 21.97	−04 17 39.9	0.219±0.022	−1.64 ± 0.05	−3.97 ± 0.18	87 ± 5
G028.39 + 00.08	18 42 51.98	−03 59 54.0	0.219±0.017	−1.41 ± 0.04	−3.27 ± 0.09	75 ± 5
G028.83 − 00.25	18 44 51.09	−03 45 48.4	0.181±0.029	−1.85 ± 0.07	−4.56 ± 0.14	87 ± 5
G028.86 + 00.06	18 43 46.22	−03 35 29.6	0.135±0.018	−4.80 ± 0.30	−5.90 ± 0.30	100 ± 10
G029.86 − 00.04	18 45 59.57	−02 45 06.6	0.161±0.020	−2.32 ± 0.11	−5.29 ± 0.16	100 ± 3
G029.95 − 00.01	18 46 03.74	−02 39 22.3	0.190±0.019	−2.30 ± 0.13	−5.34 ± 0.13	98 ± 3
G029.98 + 00.10	18 45 39.96	−02 34 32.6	0.156±0.010	−1.33 ± 0.50	−3.63 ± 0.50	109 ± 10
G030.19 − 00.16	18 47 03.07	−02 30 36.3	0.218±0.017	−1.97 ± 0.03	−3.85 ± 0.10	108 ± 3
G030.22 − 00.18	18 47 08.30	−02 29 29.3	0.235±0.013	−0.88 ± 0.03	−4.64 ± 0.22	113 ± 3
G030.41 − 00.23	18 47 40.76	−02 20 30.9	0.260±0.042	−1.90 ± 0.10	−4.10 ± 0.25	103 ± 3
G030.70 − 00.06	18 47 36.80	−02 00 54.3	0.145±0.026	−2.24 ± 0.06	−5.16 ± 0.12	89 ± 3
G030.74 − 00.04	18 47 37.73	−01 57 54.7	0.434±0.038	−4.31 ± 0.05	−3.88 ± 0.50	88 ± 3
G030.78 + 00.20	18 46 48.09	−01 48 53.9	0.145±0.028	−1.94 ± 0.06	−4.00 ± 0.15	82 ± 5
G030.81 − 00.05	18 47 46.98	−01 54 26.4	0.331±0.079	−2.35 ± 0.05	−5.66 ± 0.10	105 ± 5
G030.97 − 00.14	18 48 22.04	−01 48 30.8	0.295±0.016	−2.15 ± 0.05	−3.68 ± 1.01	77 ± 3
G031.28 + 00.06	18 48 12.38	−01 26 28.8	0.234±0.039	−2.09 ± 0.16	−4.37 ± 0.21	109 ± 3
G031.41 + 00.30	18 47 34.31	−01 12 46.7	0.267±0.029	−2.15 ± 0.05	−5.85 ± 0.07	97 ± 15
G031.58 + 00.07	18 48 41.68	−01 09 59.0	0.204±0.030	−1.88 ± 0.40	−4.84 ± 0.40	96 ± 5
G032.04 + 00.05	18 49 36.58	−00 45 45.8	0.193±0.008	−2.21 ± 0.40	−4.80 ± 0.40	97 ± 5
G033.09 − 00.07	18 51 59.41	+00 06 34.3	0.143±0.020	−2.35 ± 0.20	−5.35 ± 0.15	100 ± 5
G033.39 + 00.00	18 52 14.64	+00 24 54.4	0.136±0.022	−2.44 ± 0.05	−5.33 ± 0.14	102 ± 5
G033.64 − 00.22	18 53 32.56	+00 31 39.1	0.153±0.017	−3.18 ± 0.10	−6.10 ± 0.10	60 ± 3

combing with previous 16 sources:

Total： 42 sources

longitude range:

0° - 34°

diatance:

2.5 - 10.2 kpc

Geometry of the Scutum Arm

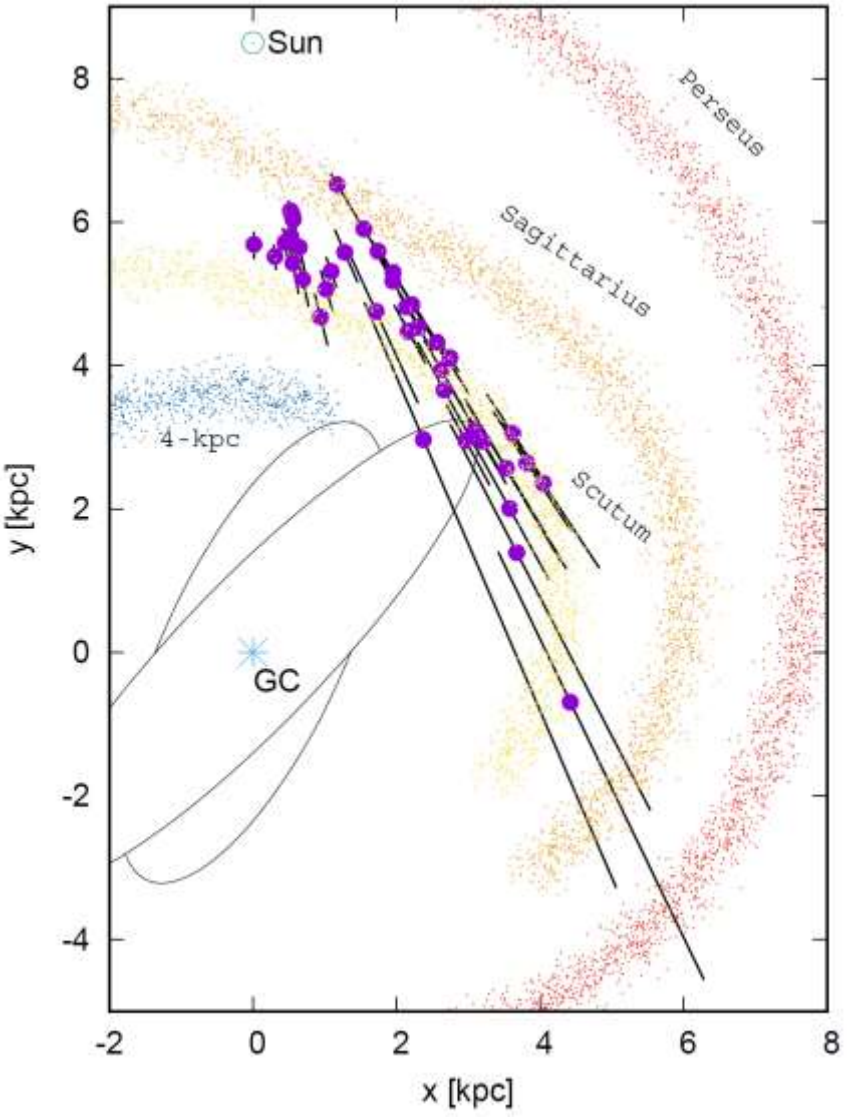

Background：
Taylor & Cordes （1993）

long bar：
Benjamin et al. (2005)
short bar:
Gerhard (2002)
Churchwell et al. (2009)

Pitch Angle of the Scutum Arm

- assuming a logarithmic spiral model
- Bayesian Markov chain Monte Carlo (McMC) fitting
- use of arm tangent point $l = 32^\circ \pm 3^\circ$ as a constraint in the fitting
- High pitch angle of the Scutum Arm: $18^\circ.7 \pm 2^\circ.9$

- Local: $11^\circ.6 \pm 1^\circ.8$ (Xu et al. 2016)
- Sagittarius: $6^\circ.9 \pm 1^\circ.6$
- Perseus: $9^\circ.4 \pm 1^\circ.4$
- Outer: $13^\circ.8 \pm 3^\circ.3$ (Reid et al. 2014)

The high pitch angle of the arm may be due to the arm's proximity to the Galactic bar!

Peculiar Motions of Massive Star Forming Regions

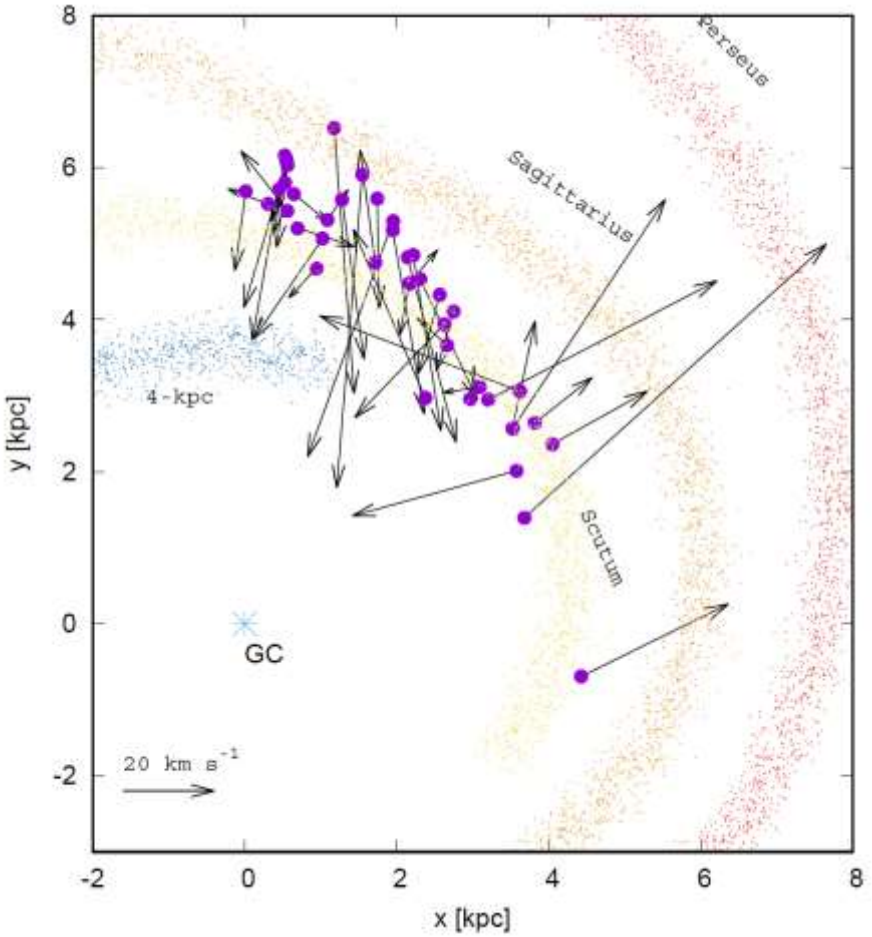

R_0 = 8.31 kpc
Θ_0 = 241 km/s

$U_\odot$ = 10.5 km/s
$V_\odot$ = 14.4 km/s
$W_\odot$ = 8.9 km/s

Reid et al., 2014

Average motions:
U = 15.4 +/- 1.3 km/s
V = 2.7 +/- 0.9 km/s
W = 1.9 +/- 0.5 km/s

The large non-circular motion may be due to the proximity of the arm to the gravitational potential of the center bar.



Thanks for your attention!